JOURNAL OF MATERIALS SCIENCE 29 (1994) 3248–3254

# Mechanical characterization of calcium-modified lead titanate ceramics by indentation methods

J. RICOTE, L. PARDO, B. JIMÉNEZ
*Instituto de Ciencia de Materiales (Sede A), CSIC, Serrano 144, 28006 – Madrid, Spain*

The microstructural dependence of the mechanical properties of Ca-modified lead titanate piezoelectric ceramics were studied. To this end, a combination of the Vickers and Knoop indentation techniques at different applied loads was used as simple method for mechanical characterization of these ceramics. The influence of porosity, grain size and tetragonal distortion on hardness, Young's modulus and toughness is discussed. An attempt to obtain internal stresses from toughness variation reveals the limitations of the method.

## 1. Introduction

Modified lead titanate ceramics are materials of interest due to their piezoelectric properties which arise from the important spontaneous polarization of their structure. This polarization is due to their high crystalline anisotropy, which on the other hand gives rise to intergranular stresses. These stresses limit their potential as electromechanical transducers. Knowledge of the influence of the material's microstructure on this effect can provide information of relevance to their piezoelectric performance.

The indentation test is a simple method to study mechanical properties, and suitable for small sample sizes. In principle, a complete mechanical characterization of the material could be carried out from indentation tests, as Knoop and Vickers hardness, indentation toughness, or critical stress intensity factor, $K_{IC}$, [1–9], Young's modulus [10], and surface stresses [11] can be estimated from these tests. However, the proper application of this technique to measure $K_{IC}$ requires determination of the crack development regime under the applied load considered [6, 7], which can only be done unambiguously by direct observation of cracks using scanning electron microscopy (SEM). Furthermore, the number of equations to determine $K_{IC}$ in the literature and their different criteria for application suggest that it is necessary to formulate them into a standardized form [8]. The majority of these equations produce a good correlation between toughness measured by indentation and by other conventional methods.

The variation of $K_{IC}$ as a function of the crack length square root, $c^{1/2}$, is the basis for calculating surface stresses [11–13]. The limitations of this method are under discussion [14, 15].

The purpose of this work is to explore the potential of the indentation method for the mechanical characterization of Ca-modified lead titanate ceramics, in order to obtain information on the microstructural dependence of their mechanical properties.

## 2. Experimental procedure

### 2.1. Materials

Ceramics were prepared with the following nominal composition [16]:

$$Pb_{1-x}Ca_x[(Co_{0.5}W_{0.5})_{0.05}Ti_{0.95}]O_3 + 1\%\ MnO$$

with $x = 0.24$, 0.26 and 0.35, PTC24/76, PTC26/74 and PTC35/65, respectively. By changing the sintering conditions, different microstructures were obtained. Disks of 15 mm diameter and 0.5–3 mm thickness were cut from sintered samples, and surfaces were polished with 0.3 μm alumina paste.

Microstructural characterization was carried out using SEM micrographs taken on these polished ceramic surfaces, previously coated with gold, using the linear intercept procedure. Quenching from 1000 °C to room temperature was necessary to enhance grain boundaries for the grain size determination.

### 2.2. Indentation techniques

Knoop and Vickers hardness were measured in a hardness meter with loads from 0.3 to 42 kg using diamond indentors and an indentation time of 35 s. Tests were carried out on unpoled ceramic samples.

Knoop and Vickers hardness values ($H_k$, $H_v$, respectively) were calculated from the well-known formulae

$$H_k(\mathrm{kg\,mm^{-2}}) = \frac{P(\mathrm{kg})}{7.028\cdot 10^{-8}\,a'^2\,(\mu m^2)}$$

$$H_v(\mathrm{kg\,mm^{-2}}) = \frac{1.854\cdot 10^6\,P(\mathrm{kg})}{d^2\,(\mu m^2)} \quad (1)$$

where $P$ is the applied load, $a'$ the longest diagonal of the Knoop indentation, and $d$ the diagonal of the Vickers indentation. Young's modulus, $E$, has been calculated from the ratio between diagonals of the Knoop indentation impression, $b/a'$ by the method described in [10].



0022–2461 

For the determination of toughness ($K_{IC}$), several formulae have been proposed [1–8] as a function of the crack length in the Vickers test, $c$. These expressions can be classified into two groups, depending on the crack geometry assumed: Palmqvist cracks and median or 'halfpenny' shaped cracks. The former appear at low loads and the latter at high loads. Some formulae are based on curve-fitting analysis of experimental data, and are independent of the crack geometry. Here we have analysed three of these expressions.

Shetty *et al.* [17] derived an equation valid in the low load or Palmqvist regime. This equation was corrected according to [8] and the indenter half angle assumed as $\theta = 68°$. As a result the following is obtained:

$$K_{IC} = \frac{0.0423}{1 - \nu^2}\left[\frac{H_v P}{l}\right]^{1/2} \quad (2)$$

where $2l = d + 2c$. The Poisson's ratio values, $\upsilon$, used in our calculations for each ceramic were obtained from measurements at the planar mode of disk-shaped piezoelectric resonators.

In [1], Evans & Charles proposed an equation valid in the median regime, from which we derive:

$$K_{IC} = 0.0235\left[\frac{3E}{H_v}\right]^{0.4}\frac{P}{c^{3/2}} \quad (3)$$

assuming the constraint factor, defined in [1], $\phi = 3$ and $H_v(\text{Pa}) = 0.47\,P(\text{N})/a^2(\text{m}^2)$, directly obtained from (1), as usually found in the literature. The parameter $a$ is the semidiagonal of the Vickers indentation impression: $a = d/2$.

Liang *et al.* [7] obtained a universal curve-fitting derived expresson:

$$K_{IC} = \frac{H_v a^{1/2}}{3\,C(\nu)}\left[\frac{3E}{H_v}\right]^{0.4}\left[\frac{c}{a}\right]^{(c/18a - 1.51)}$$

with:

$$C(\nu) = 14 - 112\left[\frac{4\nu - 0.5}{1 + \nu}\right]^4 \quad (4)$$

Equations 2 and 3 show a good ability to correlate $K_{IC}$ obtained by indentation tests and by other conventional methods, as is concluded in [9]. Furthermore, Equation 3 is studied in [9], which combines both correlating and ranking of materials in order of toughness ability. Equation 4 is not included in [9], but other curve-fitting equations show similar characteristics to Equation 3.

### 2.3. Surface stress analysis

From the values of toughness, according to [12] we have

$$K_{IC} = (K_{IC})_0 + 2\sigma_i\left[\frac{c}{\pi}\right]^{1/2} \quad (5)$$

where $(K_{IC})_0$ is the intrinsic toughness, in absence of surface stress. From this expression surface stresses, $\sigma_i$, can be calculated from the linear fitting by the least-squares method of the experimental data of $K_{IC}$ against $c^{1/2}$.

Results in [18] show that the domains tend to be oriented with the polar axis parallel to tensile applied stress. Domain reorientation under stress results in changes in relative intensities of $X$-ray diffraction (XRD) peaks. Intensities of 200 and 002 reflections were measured by an automatic X-ray powder diffractometer to check the surface stress condition of the samples. Intensity ratio of 200 and 002 reflections, $R = I_{200}/I_{002}$, is equal to 2 in a surface free of stresses.

## 3. Experimental Results

### 3.1. Microstructural and mechanical characterization

Microstructural characteristics of ceramics, grain size ($G$) and pore size ($P$) with their standard deviation ($\sigma$), as well as the percentage of porosity, are summarized in Table I, together with their tetragonal distortion of the perovskite structure ($c^*/a^*$), determined by XRD, diameter contraction during sintering, and final density determined by the Archimedes method. In 26/74 ceramics, sintering temperature and time are shown to point out the different microstructures obtained by changing these conditions (Figs 1a–c). However, tetragonal distortion depends only on the composition, decreasing with increasing calcium content.

Fig. 2 shows the typical behaviour of the Vickers hardness as a function of applied load for two ceramics of PTC26/74 sintered at 1000 °C for 5 h (A2) and 1050 °C for 3 h (B1). It can be seen that there is a high scattering of the results for low loads. This fact is due, to some extent, to difficulties in measurement on reduced indentation impressions. However, there seems to be an anomalous increase of Vickers hardness with applied load, reaching a maximum and then a decrease with a trend to stability for higher loads. This stability of hardness seems to be in relation to the appearance of well-defined cracks.

Table II shows the mean values of hardness (Knoop and Vickers) over the applied loads, and Young's modulus, $E$. Accuracy of the method used for the determination of $E$ depends on the ratio $H_k/E$ [10], and is also shown in Table II. Two different methods were used in the calculation of $E$ values appearing in this table. When $H_k$ was found to be almost independent of $P$, the mean values of $H_k$ and $b/a'$ were used to obtain $E$, otherwise $E$ was calculated for each $P$ and then a mean value of $E$ was obtained.

A limitation of the indentation method for coarse-grained ceramics arises from the effect of grain size on crack length [5, 9]. When the mean grain size is much smaller than the indentation diagonal $d$, the edges will be undulating and the length of the cracks, which follow grain boundaries, will be asymmetric. This is the case for the majority of ceramics studied. For grain size of the order of $d$, the crack pattern is severely disrupted by localized grain-size events. Disruptions of crack pattern increase with increasing grain size, until $G \gg d$, when these effects disappear. For this reason, indentations on C1 ceramic have broken edges

TABLE I Microstructural characterization of PTC ceramics, showing the tetragonal distortion, $c^*/a^*$; density, ρ; diameter contraction, grain and pore sizes together with the percentage of porosity for ceramics with different compositions and sintering conditions.

| PTC Ceramic | $c^*/a^*$ | ρ (g cm$^{-3}$) | Diameter contraction (%) | Grain size | | Pore size | | Porosity (%) |
|---|---|---|---|---|---|---|---|---|
| | | | | $G$(μm) | σ(μm) | $P$(μm) | σ(μm) | |
| Ca/Pb = 24/76 | | | | | | | | |
| A | 1.040 | 6.76 | 14.72 | 2.98 | 1.41 | 1.76 | 1.21 | 12–17 |
| B | 1.041 | 6.55 | 14.45 | 4.18 | 1.82 | 2.03 | 2.51 | 18–20 |
| Ca/Pb = 26/74 | | | | | | | | |
| 1000 °C–3 h A1 | 1.037 | 6.77 | 10.01 | 2.99 | 1.35 | 1.61 | 1.05 | 16 |
| 1000 °C–5 h A2 | 1.038 | 6.76 | 10.56 | 3.04 | 1.42 | 1.60 | 1.00 | 16–19 |
| 1050 °C–3 h B1 | 1.038 | 6.73 | 12.93 | 3.60 | 3.41 | 1.59 | 0.86 | 6–8 |
| 1050 °C–5 h B2 | 1.038 | 6.64 | 13.25 | 4.30 | 1.92 | 1.95 | 1.17 | 2–6 |
| 1100 °C–3 h C1 | 1.038 | 6.55 | 11.84 | 5.95 | 0.99 | 4.70 | 2.70 | 10–11 |
| 1100 °C–5 h C2 | 1.038 | 6.40 | 11.69 | 4.81 | 2.42 | 5.04 | 4.60 | 15–19 |
| Ca/PB = 35/65 | | | | | | | | |
| A | 1.018 | 6.35 | 15.62 | 2.41 | 1.28 | 2.42 | 1.93 | 23–27 |
| B | 1.017 | 6.33 | 12.45 | 2.40 | 1.08 | 1.90 | 1.49 | 25–30 |

(Fig. 3), and instead of four symmetrical cracks, there is crack branching and cracks occurring from the sides of the indentation. A similar effect was observed by Yamamoto *et al.* [13] on PTC ceramics with a grain size above 3.8 μm. Despite this effect, hardness values were obtained for C1 ceramics. This microstructural effect of deformation on indentation impressions is higher for the minor diagonal in Knoop indentations; therefore, results of $E$, as well as $K_{IC}$, were not reliable, and are not shown in Tables II–IV. On the other hand, the rest of the ceramics studied, whose grain size is lower, have acceptable crack patterns.

The dependence of the ratio of the crack to indentation sizes, $c/a$, with respect to the applied load, $P$, is shown in Fig. 4. Experimental data for these parameters were fitted as a function of $P$, and then the quotient between the fitted expressions was plotted. Using the numerical criteria, $c/a > 2$ for cracks in median regime, it can be observed that the appearance of this kind of crack depends on the porosity of the ceramic. The median regime cracks appear at a higher applied load the higher the porosity.

Fig. 5 shows the typical behaviour of toughness, calculated from Equation 3 as a function of applied load for the same two ceramics as in Fig. 2: PTC26/74 A2 and B1. Although unacceptable crack patterns were excluded, the scattering of the crack length measurements is important, resulting in a large scattering of the toughness results. Mean values at each load of $K_{IC}$ obtained from Equation 3 for these two ceramics are plotted against $c^{1/2}$ in Fig. 6. Linear fitting was carried out only for the experimental values that hold $c/a > 2$ (median crack regime). As was also seen in [11], a different behaviour for the two crack regimes is observed. Toughness increases with increasing $c^{1/2}$ for values obtained from low load cracks (Palmqvist), whereas it decreases for values from higher load cracks (median).

Mean toughness values obtained from Equations 2, 3 and 4 are summarized in Table III. Calculations were made in the range of validity of each equation. For some ceramics there are not enough data within the appropriate crack regime, and it was not possible to obtain toughness from either Equation 2 or 3.

## 3.2. Surface stress analysis

One requirement in order to obtain reliable results from indentation techniques is a sample surface free of stresses. Surface grinding, part of the ceramic processing, produces a compressive surface stress. In [19] it is suggested that annealing after polishing may be used to remove this stress.

Table IV summarizes the values of $I_{200}/I_{002}$ ratio for the different states of the surface of B1 during sample preparation. These are the surface after grinding, after polishing with 0.3 μm alumina paste, and after annealing at 350 °C for 15 min. The $I_{200}/I_{002}$ ratio for the indented samples, mean hardness and toughness values over the applied loads in the median crack regime are also included for comparison.

The results in Table IV show that the ground surface presents a ratio well below the theoretical value for the absence of preferential orientation of the lattice, $R = 2$. This indicates that the grinding process introduces orientation by generation of mechanical stresses in the surface. However, it is not necessary to use an annealing process after polishing to eliminate these stresses. According to these results, the values of hardness and toughness obtained for samples with and without annealing are the same. Consequently, the data on $K_{IC}$ presented in this work and obtained from polished and non-annealed samples can be used to estimate (by the method described in [11]) the internal stresses of the ceramics arising from the tetragonal distortion of the perovskite structure, and the different degrees of compactness of the grains in each ceramic, because they are the main cause of remanent surface stress after the elimination of the stress caused by surface grinding.

The results of the $K_{IC}$ against $c^{1/2}$ linear regression analysis for PTC26/74 ceramics are shown in Table V, together with their regression factors, $r^2$. The mean toughness, obtained from Equations 2, 3 and 4, and

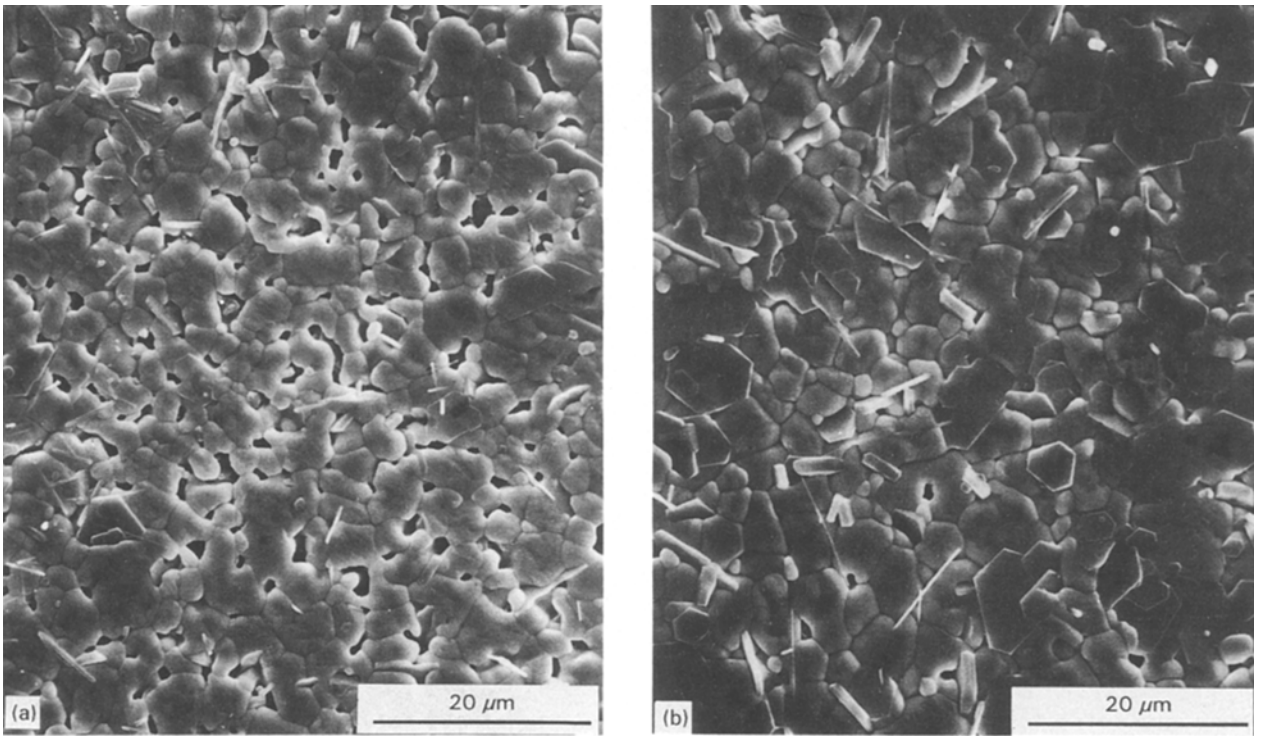


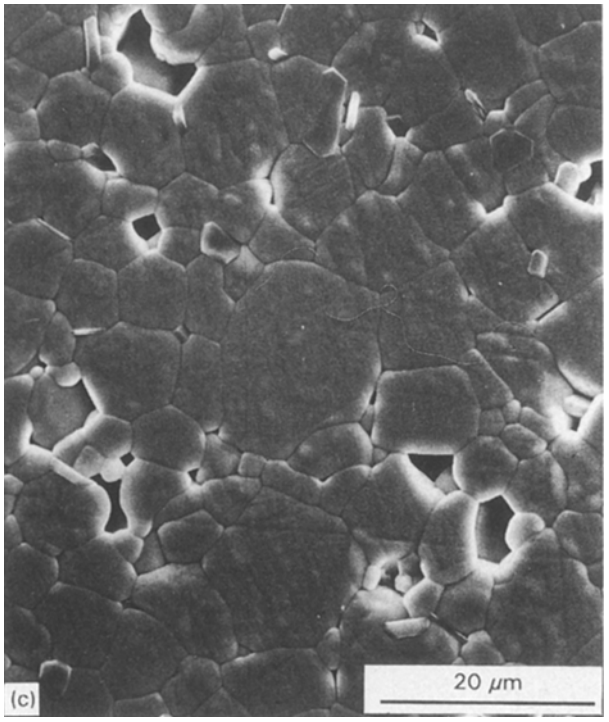


*Figure 1* SEM micrographs of PTC26/74 ceramics: (a) A1, (b) B1, (c) C1.

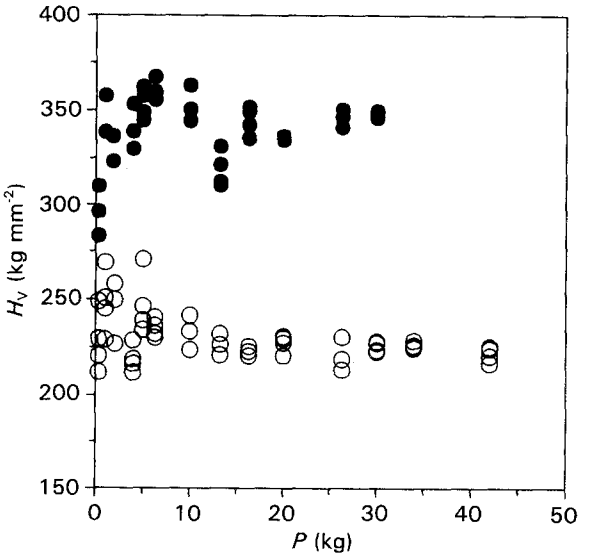


*Figure 2* Vickers hardness as a function of the applied load, $P$, for two PTC26/74 ceramics: ○, A2 and ●, B1.

the mean crack length over the measurements at each applied load, were used in linear fitting. Calculations were carried out in the range of validity of each equation.

## 4. Discussion

From the results shown above, some relations between mechanical properties and microstructure for Ca-modified $PbTiO_3$ ceramics can be deduced. Ceramic porosity and grain size seem to be important factors in the mechanical behaviour of these ceramics.

In two-phase systems the overall Young's modulus is intermediate between high- and low-modulus components [20]. This can also be assumed as valid for hardness. A porous ceramic is a two-phase material, in which one phase has approximately zero stiffness and zero hardness. As a result, Vickers and Knoop hardness and Young's modulus decrease with increasing porosity. Results obtained for PTC ceramics, discussed below, show the same relations.

Mean values of Knoop and Vickers hardness are similar for each sample, thus hardness behaviour is discussed regardless of the indenter used in the measurement. Comparison between results shown in Tables I and II shows that hardness decreases with increasing ceramic porosity for samples with the same

TABLE II Mechanical properties of PTC ceramics, showing also the accuracy of the method used for the determination of $E$.

| PTC Ceramics | Knoop hardness, $H_k$ (GPa) | Young's modulus, $E$ (GPa) | $H_k/E$ | Accuracy of method | Vickers hardness, $H_v$ (GPa) |
|---|---|---|---|---|---|
| 24/76 A | 3.2 ± 0.7 | 142 ± 46 | 0.02 | > 10% | 3.4 ± 0.5 |
| 24/76 B | 2.3 ± 0.4 | 65 ± 13 | 0.04 | < 10% | 2.8 ± 0.6 |
| 26/74 A1 | 1.9 ± 0.2 | 69 ± 17 | 0.03 | > 10% | 2.0 ± 0.1 |
| 26/74 A2 | 2.0 ± 0.3 | 137 ± 43 | 0.01 | > 10% | 2.3 ± 0.4 |
| 26/74 B1 | 3.0 ± 0.5 | 147 ± 98 | 0.02 | > 10% | 3.3 ± 0.5 |
| 26/74 B2 | 3.0 ± 0.2 | 109 ± 32 | 0.03 | > 10% | 3.3 ± 0.4 |
| 26/74 C1 | 2.5 ± 0.5 | – | – | – | 2.7 ± 0.6 |
| 26/74 C2 | 2.1 ± 0.3 | 107 ± 43 | 0.02 | > 10% | 2.5 ± 0.6 |
| 35/65 A | 3.2 ± 0.4 | 115 ± 28 | 0.03 | > 10% | 3.3 ± 0.7 |
| 35/65 B | 1.8 ± 0.3 | 96 ± 39 | 0.02 | > 10% | 1.7 ± 0.2 |

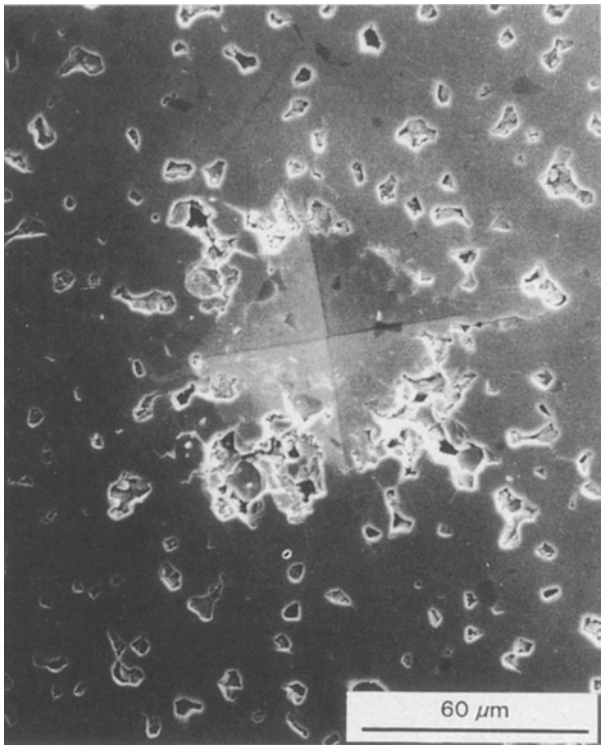


*Figure 3* Micrograph of a typical indentation on C1 ceramic, at test load $P = 1$ kg.

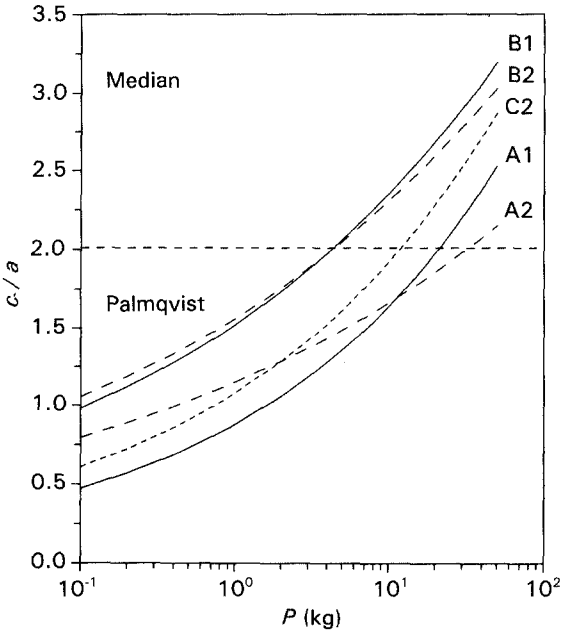


*Figure 4* Plot of the crack-to-indentation-size ratio, $c/a$, against the applied load, $P$, for PTC26/74 ceramics with different porosity.

composition. In Fig. 7, Vickers hardness is plotted as a function of the percentage of porosity of the samples, showing error bars. Linear fitting is carried out for each composition to underline the different behaviour of materials with different tetragonal distortion. It can be seen that hardness values for PTC24/76 and PTC26/74 are very close. Meanwhile, the highest value of hardness was measured for PTC35/65 A, in spite of the high porosity of these samples. Therefore, tetragonal distortion is a factor to be taken into account in hardness behaviour of PTC ceramics, as pointed out in [12]. The influence of porosity on Young's modulus is inferred from the results on PTC35/65 A and B, which have close values of grain size. Young's modulus is higher the lower the ceramic porosity, in agreement with results shown in [20].

Values of $K_{IC}$ from Equation 4, for PTC35/65 A and B as shown in Table III, suggest that toughness increases with increasing ceramic porosity. An explana-

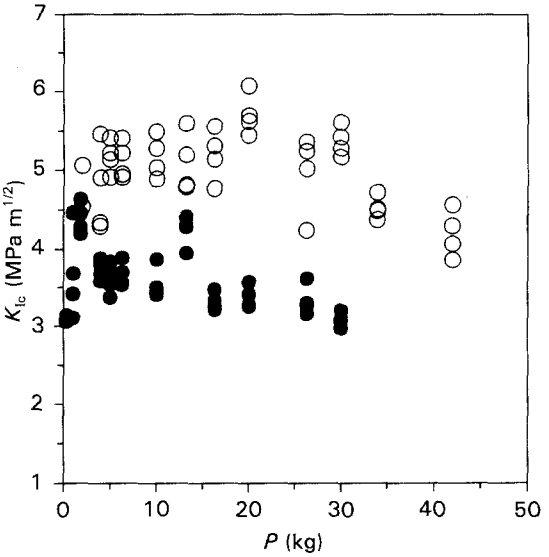


*Figure 5* Toughness, calculated from Equation 3, as a function of the applied load for PTC26/74 ○, A2, and ●, B1 ceramics.

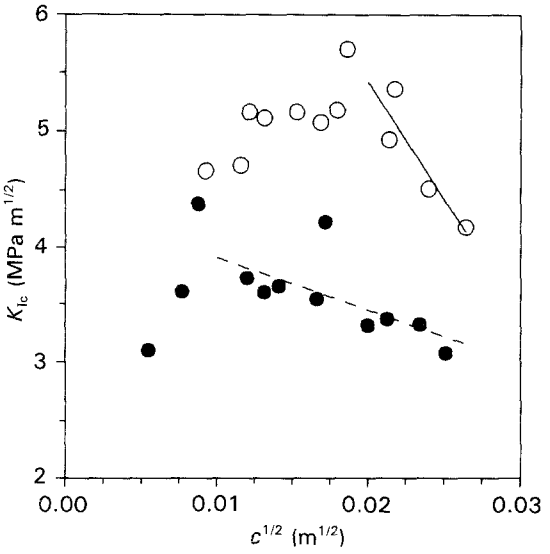


*Figure 6* Mean values of toughness at each applied load, calculated from Equation 3, as a function of the square root of crack length, $c^{1/2}$, for PTC26/74 ○, A2 and ●, B1 ceramics.

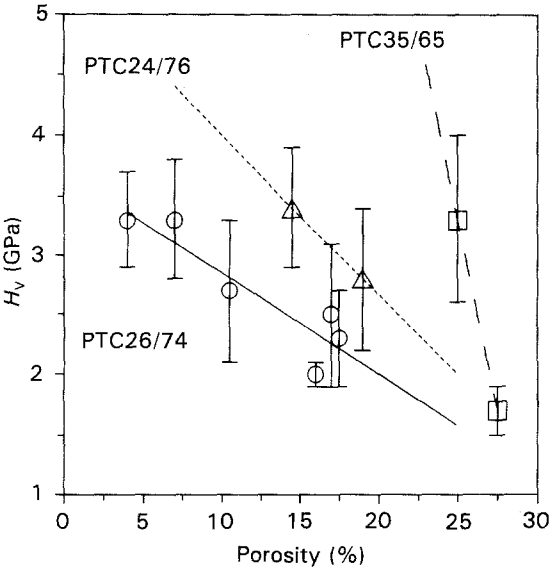


*Figure 7* Vickers hardness as a function of the porosity, showing error bars.

TABLE III Mean toughness values of PTC ceramics obtained from different equations, together with the range of $c/a$.

| PTC Ceramics | Toughness, $K_{IC}$ (MPa m$^{1/2}$) | | | $c/a$ range |
|---|---|---|---|---|
| | Equation 2 | Equation 3 | Equation 4 | |
| 24/76 A | 2.3 ± 0.6 | 3.9 ± 0.7 | 2.4 ± 0.6 | 1.4–2.8 |
| 24/76 B | 2.2 ± 0.5 | – | 1.9 ± 0.4 | 1.3–1.9 |
| 26/74 A1 | – | 3.3 ± 0.4 | 1.7 ± 0.1 | 1.9–2.3 |
| 26/74 A2 | 2.2 ± 0.5 | 4.3 ± 0.5 | 2.5 ± 0.6 | 1.4–2.4 |
| 26/74 B1 | 1.8 ± 0.2 | 3.5 ± 0.9 | 2.0 ± 0.6 | 1.4–3.2 |
| 26/74 B2 | – | 3.1 ± 0.8 | 1.8 ± 0.5 | 2.4–3.0 |
| 26/74 C2 | – | 3.6 ± 0.2 | 2.0 ± 0.5 | 1.8–2.6 |
| 35/65 A | 1.7 ± 0.2 | 3.0 ± 0.6 | 2.1 ± 0.6 | 1.4–2.3 |
| 35/65 B | 1.7 ± 0.7 | – | 3.3 ± 1.4 | 1.3–1.8 |

tion for which could be that cracks are stopped by pores. However, an upper limit of porosity is expected for the validity of this behaviour. Therefore, a moderate presence of pores may have a crack-blocking function. If crack length decreases, toughness increases, in agreement with the dependence on $c$ shown clearly in Equations 2 and 3, and also seen in Equation 4.

The influence of grain size on mechanical properties of PTC ceramics has also been studied. PTC26/74 B1 and B2, and PTC26/74 A2 and C2 are suitable examples for this study, because they have similar porosity but a different grain size. From these results it follows that hardness is independent of grain size within the range studied, and Young's modulus seems to decrease with increasing grain size. Concerning toughness results, a decrease is observed as grain size increases.

An interpretation of toughness behaviour can be found in the fact that a proportionality between fracture stress, $\sigma_f$, and $K_{IC}$ follows the Griffith–Orowan–Irwin analysis of fracture mechanics [21] and therefore these parameters are expected to behave similarly. Experimental data for $\sigma_f$ on polycrystalline materials has been usually described by one of these

TABLE IV $I_{200}/I_{002}$ ratio values for the different surface states of B1 sample together with mean $H_v$ and toughness.

| Sample | $R = I_{200}/I_{002}$ | | | | Vickers hardness, $H_v$ (GPa) | Toughness, $K_{IC}$ (MPa m$^{1/2}$) |
|---|---|---|---|---|---|---|
| | Ground | Polished | Annealed | Indented | | |
| Non-annealed | 1.04 | 1.87 | – | 1.68 | 3.3 ± 0.3 | 2.9 ± 0.4 |
| Annealed | 0.87 | 2.03 | 1.92 | 1.81 | 3.3 ± 0.7 | 3.2 ± 0.1 |

TABLE V Values of $A$ (MPa) and $B$ (MPa m$^{1/2}$) for the linear fitting $K_{IC} = Ac^{1/2} + B$, together with the regression factor, $r^2$.

| PTC 26/74 | Equation (3) | | | Equation (4) | | | Equation (2) | | |
|---|---|---|---|---|---|---|---|---|---|
| | $A$ | $B$ | $r^2$ | $A$ | $B$ | $r^2$ | $A$ | $B$ | $r^2$ |
| A1 | – 67 | 4.8 | 0.8724 | – 22 | 2.2 | 0.4597 | – | – | – |
| A2 | – 198 | 9.4 | 0.8191 | 12 | 2.3 | 0.0909 | 46 | 1.5 | 0.880 |
| B1 | – 46 | 4.4 | 0.4218 | – 1.9 | 2.0 | 0.0035 | 142 | 0.8 | 0.761 |
| B2 | – 28 | 3.7 | 0.0761 | – 7.9 | 1.9 | 0.0137 | – | – | – |
| C2 | – 27 | 4.1 | 0.2405 | – 56 | 3.2 | 0.8503 | – | – | – |

relations [20], or a combination of them:

$$\sigma_f = \sigma_0 + k_1 G^{-1/2} \quad \text{Petch relation}$$

$$\sigma_f = k_2 G^{-1/2} \quad \text{Orowan relation}$$

where $k_1$ and $k_2$ are constants depending on the material, and $\sigma_0$ is the characteristic strength. From these well-known expressions, $\sigma_f$ and as a consequence $K_{IC}$, are expected to decrease with increasing grain size as our results of $K_{IC}$ confirm.

A series of recent works [22, 23] point out that toughness is not a material constant and examine the *R*-curve behaviour, i.e. the increase of toughness with the crack-size scale. Although it seems to be related with the results in this paper, we are dealing with the stress intensity factor or toughness obtained by indentation methods. *R*-curve behaviour is studied by indentation–strength methods, which involves several factors influencing the crack evolution that we cannot take into account. In fact $K_{IC}$ is considered as one of these factors. Therefore, the conclusions of these works are not considered in this study.

Results shown in Table V summarize attempts to calculate the ceramic internal stresses on the basis of the $K_{IC}$ variation as a function of $c^{1/2}$. Although values of internal stresses and intrinsic toughness are of the same magnitude as previously reported values [12] in modified lead titanate ceramics, it is observed that results depend on the $K_{IC}$ expression used, and also changes in sign of the slope are found. These could be understood as changes in sign of the application of internal stresses (tensile or compressive). However, recent works [5] pointed out that the sign of the slope cannot be used as an indicator unless stress state is known by other methods. As our results are not conclusive, we can suggest a limitation of the method for ceramics that have a non-negligible residual porosity, such as the samples studied, in addition to the criticisms that the method itself has received [14, 15].

## 5. Conclusions

On microstructurally well characterized ceramic samples of Ca-modified lead titanate, a combination of Knoop and Vickers indentation tests has been used to establish correlations between the mechanical properties of these materials and their microstructure. The results are listed below.

1. Knoop and Vickers hardness of PTC ceramics decrease with increasing ceramic porosity and are independent of grain size. Tetragonal distortion is another factor to be taken into account, giving the highest value of hardness for the PTC35/65 ceramics, which show the lowest values of tetragonal distortion.

2. Young's modulus of the ceramics studied is higher the lower the ceramic porosity.

3. The median crack regime in PTC ceramics appears at higher applied load as the ceramic porosity increases. This is an important factor in toughness calculations, because different equations have to be used depending on the crack regime.

4. X-ray diffraction data reveals that for the measurement of $K_{IC}$ by indentation methods, annealing treatment is unnecessary, as careful polishing of the samples removes the surface stresses caused by grinding.

5. Toughness seems to increase as ceramic porosity increases, as pores act as a crack-blocking mechanism in ceramics with moderate porosity. On the other hand, toughness decreases with increasing grain size in agreement with the well known fact that fracture stress is lower the higher the grain size in polycrystalline materials.

6. The variation of $K_{IC}$ with $c^{1/2}$ leads to a calculation of internal stresses and intrinsic toughness values that depends on the expression used for $K_{IC}$. In-conclusive results in the calculation of internal stresses by indentation method suggest a limitation due to the non-negligible residual porosity of the samples.

## Acknowledgements

The authors wish to thank C. Fandiño and F. Díaz for material preparation, and D. Gómez of the "Centro Nacional de Microelectrónica" for the SEM micrographs of the samples. This work has been financed by the Spanish CICYT (project MAT88-0164).

## References

1. A. G. EVANS and E. A. CHARLES, *J. Amer. Ceram. Soc.* **59** (1976) 371.
2. B. R. LAWN and M. W. SWAIN, *J. Mater. Sci.* **10** (1975) 113.
3. B. R. LAWN and E. R. FULLER, *ibid.* **10** (1975) 2016.
4. A. G. EVANS and T. R. WILSHAW, *Acta Metall.* **24** (1976) 939.
5. G. R. ANSTIS, P. CHANTIKUL, B. R. LAWN and D. B. MARSHALL, *J. Amer. Ceram. Soc.* **64** (1981) 533.
6. Z. LI, A. GHOSH, A. S. KOBAYASHI and R. C. BRADT, *ibid.* **72** (1989) 904.
7. K. M. LIANG, G. ORANGE and G. FANTOZZI, *J. Mater. Sci.* **25** (1990) 207.
8. C. B. PONTON and R. D. RAWLINGS, *Mater. Sci. Technol.* **5** (1989) 865.
9. *Idem, ibid.* **5** (1989) 961.
10. D. B. MARSHALL, T. NOMA and A. G. EVANS, *Comm. Amer. Ceram. Soc.* October (1982) C-175.
11. D. B. MARSHALL and B. R. LAWN, *J. Amer. Ceram. Soc.* **60** (1977) 86.
12. T. YAMAMOTO, H. IGARASHI and K. OKAZAKI, *ibid.* **66** (1983) 363.
13. *Idem. Ceram. Int.* **11** (1985) 75.
14. D. J. GREEN, *J. Mater. Sci.* **20** (1985) 4239.
15. Y. IKUMA and A. V. VIRKAR, *ibid.* **20** (1985) 4241.
16. L. DEL OLMO, C. FANDIÑO, J. I. PINA, C. ALEMANY, J. MENDIOLA, L. PARDO, B. JIMENEZ and E. MAURER, Patente Española de Invención #555469 (1986).
17. D. K. SHETTY, I. G. WRIGHT, P. N. MINCER and A. H. CLAUER, *J. Mater. Sci.* **20** (1985) 1873.
18. E. C. SUBBARAO, M. C. McQUARRIE and W. R. BUESSEM, *J. Appl. Phys.* **28** (1957) 1194.
19. Y. IKUMA and A. V. VIRKAR, *J. Mater. Sci.* **19** (1984) 2233.
20. R. W. DAVIDGE, "Mechanical Behaviour of Ceramics", 1st edn (Cambridge University Press, Cambridge, 1979) p. 27.
21. W. D. KINGERY, H. K. BOWEN and D. R. UHLMANN, "Introduction to Ceramics", 2nd edn (Wiley, New York, 1976) p. 785.
22. P. CHANTIKUL, S. J. BENNISON and B. R. LAWN, *J. Amer. Ceram. Soc.* **73** (1990) 2419.
23. S. J. BENNISON and B. R. LAWN, *Acta Metall.* **37** (1989) 2659.

*Received 22 June*
*and accepted 10 November 1993*